7-Rhamnosylated Flavonols Modulate Homeostasis of the Plant Hormone Auxin and Affect Plant Development[*]

Benjamin M. Kuhn[‡1,2], **Sanae Errafi**[‡1], **Rahel Bucher**[§], **Petre Dobrev**[¶], **Markus Geisler**[‖], **Laurent Bigler**[§],
Eva Zažímalová[¶], and **Christoph Ringli**[‡3]

From the [‡]*Department of Plant and Microbial Biology, University of Zurich, 8008 Zurich, Switzerland, the* [§]*Department of Chemistry, University of Zurich, 8057 Zurich, Switzerland, the* [¶]*Institute of Experimental Botany, Academy of Sciences of the Czech Republic, 165 02 Prague 6, Czech Republic, and the* [‖]*Department of Biology, University of Fribourg, 1700 Fribourg, Switzerland*

Flavonols are a group of secondary metabolites that affect diverse cellular processes. They are considered putative negative regulators of the transport of the phytohormone auxin, by which they influence auxin distribution and concomitantly take part in the control of plant organ development. Flavonols are accumulating in a large number of glycosidic forms. Whether these have distinct functions and diverse cellular targets is not well understood. The *rol1-2* mutant of *Arabidopsis thaliana* is characterized by a modified flavonol glycosylation profile that is inducing changes in auxin transport and growth defects in shoot tissues. To determine whether specific flavonol glycosides are responsible for these phenotypes, a suppressor screen was performed on the *rol1-2* mutant, resulting in the identification of an allelic series of *UGT89C1*, a gene encoding a flavonol 7-O-rhamnosyltransferase. A detailed analysis revealed that interfering with flavonol rhamnosylation increases the concentration of auxin precursors and auxin metabolites, whereas auxin transport is not affected. This finding provides an additional level of complexity to the possible ways by which flavonols influence auxin distribution and suggests that flavonol glycosides play an important role in regulating plant development.

Flavonoids are secondary metabolites produced via the phenylpropanoid pathway (1), and they serve different functions such as protection from UV irradiation (2), plant-microbe interaction (3), regulation of levels of reactive oxygen species (4), inhibition of cell cycle, and control of cell growth (5, 6). In addition, they are also thought to influence transcriptional and signaling processes (7–9). A major role of flavonols, a subgroup of flavonoids, appears to be the modification of auxin-related processes due to their property of modulating auxin transport (10–14). In some tissues, auxin is transported from cell to cell in a polarized fashion, operated mainly via auxin transporters of the ABCB, AUX1/LAX, and PIN families (15, 16). Flavonoids bind to and inhibit the auxin transport proteins ABCB1 and ABCB19 (17) and interfere with the interaction of these two proteins with the immunophilin-like protein, FKBP42/TWISTED DWARF1 (18). Recent data show that the pinoid kinase, which influences polar localization of PIN proteins (19) and ABCB transport activity, is a likely target of flavonol action (20). The accumulation of flavonols is altered in the *pin2* mutant, the agravitropic phenotype of which can be partially complemented by exogenous flavonols due to their ability to modify expression of *PIN* genes (21–23). Hence, flavonols and auxin are able to mutually influence each other, confirming a functional interdependence in their biological activity.

Flavonoid biosynthesis is well characterized, and a number of mutants affected in the enzymes committed to the different steps have been identified in *Arabidopsis thaliana* (1) (Fig. 1). These lines frequently show a pale yellow seed coat due to the absence of proanthocyanidins and were thus named *transparent testa* (*tt*) mutants (24). Flavonols are produced from dihydroflavonols via the activity of the flavonol synthase, and thus represent a side branch of the flavonoid biosynthesis pathway. In *Arabidopsis*, the flavonols kaempferol, quercetin, and isorhamnetin are glycosylated by one or several sugars, mainly Glc, Rha, and rarely Ara, at the C3 and C7 position of the flavonol backbone (25, 26) through the function of UDP-dependent glycosyltransferases (UGTs),[4] some of which have been identified (8, 26–29). The biological relevance of flavonol glycosylation remains controversial. *In vitro* experiments show activity of flavonol aglycones, suggesting that these are the compounds active in modulating polar auxin transport (10, 17, 18, 20). However, the identification of mutant phenotypes induced by changes in the flavonol glycosylation profile suggests function for at least some flavonol glycosides (30, 31).

Of the major auxin (indole-3-acetic acid; IAA) produced by plants, only a minor fraction of ~1% exists in this active form. Auxin can be conjugated to amino acids and/or sugars (mainly Glc in *Arabidopsis*) for storage in an inactive form or as an initial step for degradation (32, 33). Indole-3-acetyl-alanine (IAA-Ala) and indole-3-acetyl-leucine (IAA-Leu) are readily hydrolyzable, resulting in active free IAA, whereas indole-3-

[4] The abbreviations used are: UGT, UDP-dependent glycosyltransferases; K-R-3-R-7, kaempferol-3-*O*-7-*O*-rhamnoside; IAA, indole-3-acetic acid; IAA-Glc, IAA-glucose; IAA-Asp, IAA-aspartate; IAA-Glu, IAA-glutamate; oxIAA, 2-oxindole-3-acetic acid; oxIAA-Glc, oxIAA-glucose; IAN, indole-3-acetonitrile; EMS, ethyl methanesulfonate; ESI, electrospray ionization; 1-NAA, 1-naphthalene acetic acid; FLS, flavonol synthase.
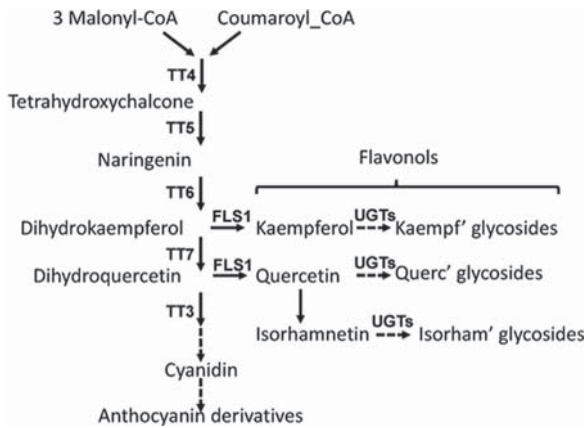
FIGURE 1. **Overview of flavonoid biosynthesis.** The phenylpropanoid pathway leads to the synthesis of flavonoids. These encompass a number of different compounds, not all of which are indicated in this scheme. Enzymes leading to the synthesis of flavonols (kaempferol, quercetin, isorhamnetin) are indicated. TT (transparent testa) proteins were identified based on the pale brown phenotype of seeds of corresponding mutant lines. *FLS1*: flavonol synthase 1, the predominant FLS protein in *Arabidopsis*. *UGTs*: UDP-dependent glycosyltransferases needed for the glycosylation of flavonols.

acetyl-aspartate (IAA-Asp) and indole-3-acetyl-glutamate (IAA-Glu) remain largely stable, suggesting that the dynamics of the reversible (de-)conjugation are decisive in regulating the pool of active auxin. Auxin homeostasis can be affected by mutations in loci involved in auxin (de-)conjugation, and multiple mutations in these loci can induce auxin-related phenotypes ((Ref. 34) and references therein). In *Arabidopsis*, the most abundant degradation products of auxin are produced via oxidation, resulting predominantly in oxIAA (2-oxindole-3-acetic acid) and oxIAA-Glc (2-oxindole-3-acetyl-glucose, glucosyl-ester of oxIAA) (35, 36). This oxidation contributes to the formation of auxin gradients (37) that are crucial for auxin-driven organ development (38 – 41). oxIAA levels are increased in the flavonoid-deficient *tt4* mutant but decreased in the flavonol over-accumulator *tt3* (42). This correlation suggests that the anti-oxidant activity of flavonols (4) influences auxin degradation.

The *rol1-2* (*repressor of lrx1*) mutant is affected in one of three *RHM* genes, *RHM1*, encoding rhamnose synthase, which converts UDP-Glc to UDP-Rha (43). The *rol1-2* mutant was identified in a screen for alterations in cell wall structures and shows modifications in the Rha-rich cell wall component pectin (43). In addition, *rol1-2* also shows changes in the flavonol glycosylation profile, mainly a reduction in the degree of rhamnosylation, whereas the overall quantity of flavonols is not affected (30, 44). This confirms the importance of *RHM1*, which is co-expressed with genes important for flavonol biosynthesis (26) and for flavonol glycosylation. *rol1-2* seedlings are characterized by shorter roots and root hairs than in the wild type. The *rol1-2* seedling shoot develops deformed trichomes and hyponastic cotyledons with brick-shaped pavement cells, whereas the wild type develops regular trichomes and epinastic cotyledons with puzzle-shaped jigsaw-like pavement cells (30, 43). There is no obvious growth defect detectable in *rol1-2* adult plants, presumably due to the functional redundancy among the three *RHM* genes (45).

The short root phenotype of the *rol1-2* mutant is most likely induced by the changes in pectin structures (43). By contrast, the aberrant shoot phenotype of the *rol1-2* mutant is connected to the altered flavonol composition. Mutations affecting steps in flavonoid biosynthesis (Fig. 1) upstream of flavonols such as *tt4* or *tt6*, mutations in the *flavonol synthase* (*FLS1*), or mutations in a positive regulator of flavonol biosynthesis encoded by *MYB111* all suppress *rol1-2*, resulting in wild type-like shoot development, whereas root development is comparable with the *rol1-2* single mutant (30, 44). A mutation in *TT7*, blocking quercetin accumulation, or any step farther downstream in the pathway has no effect on the *rol1-2* shoot phenotype (30, 44). Together, these findings suggest that the *rol1-2* phenotype is induced by the accumulation of flavonol glycosides that interfere with proper plant development and that kaempferols are sufficient to induce this defect. Yin *et al.* (31) have shown that the dwarf growth phenotype of the flavonoid 3-*O*-glucosyltransferase mutant *ugt78d2* correlates with the over-accumulation of 3-*O*-7-*O*-rhamnosylated kaempferol (K-R-3-R-7), and interfering with K-R-3-R-7 biosynthesis suppresses the growth defect of the *ugt78d2* mutant. By contrast, the flavonol species inducing the *rol1-2* phenotype is most likely not K-R-3-R-7, because this compound is present in lower amounts than in the wild type. Thus, it is likely that several flavonol glycosides can have an effect on plant development. Both *rol1-2* and *ugt78d2* show changes in auxin concentration or transport activity. For *rol1-2*, it was shown that auxin transport is reverted to wild-type levels when blocking flavonol accumulation (44), thus indicating that flavonols do interfere with auxin distribution.

Aiming at the identification of flavonol glycosides that induce the *rol1-2* phenotype, EMS-induced suppressor mutants of *rol1-2* were selected for specific changes in flavonol glycosylation. Several alleles of the 7-*O*-rhamnosyltransferase locus *UGT89C1* were identified. The auxin transport activity in *rol1-2* is not changed by a *ugt89c1* mutation, but the levels of auxin conjugates and catabolites are strongly increased in the *ugt89c1* mutant background. This indicates that flavonols affect not only auxin transport but also auxin turnover, and in this way modify auxin homeostasis.

Experimental Procedures

Plant Material, Growth Conditions, EMS Mutagenesis, and Mutant Screen—All lines described in this study are in the Col-0 genetic background. The *rol1-2* allele and *fls1-3* allele used in this study are described elsewhere (43, 44). For all analyses described, the *ugt89c1-3* nonsense allele was used. Seeds were surface-sterilized with 1% sodium hypochlorite, 0.03% Triton X-100, plated on half-strength Murashige and Skoog medium containing 0.6% Phytagel, 2% sucrose, 100 μg/ml *myo*-inositol, stratified for 4 days at 4 °C, and grown in a vertical orientation in a 16-h light, 8-h dark cycle at 22 °C. For propagation and crossings, 10-day-old plants were transferred to soil, grown in a 16-h light, 8-h dark cycle at 22 °C, and irradiated with white light (Biolux, Osram). The EMS screen was performed as described (44), and 75,000 M2 seedlings were screened for a suppressed *rol1-2* mutant phenotype. All *ugt89c1* alleles were backcrossed at least three times to Col-0 and *rol1-2* prior to analysis. Plant transformation was done as

described (43), and transgenic plants were selected with BASTA (10 μg/ml).

DNA Constructs, Plant Transformation, and Molecular Markers—For the *UGT89C1* complementation construct, the *UGT89C1* genomic clone was PCR-amplified with the primers *F7RT_PC* 5′-GGCGCGCCAGACTACAGTTTGGCTAAC-CAG-3′ and *F7RT_R3C* 5′-TGAACCGCGTGTGTAATGT-ATC-3′, encompassing 1.5-kb promoter, 1.3-kb coding sequence, and 0.35-kb terminator sequence. The resulting fragment (*UGT89C1:UGT89C1*) was cloned into pGEM-T Easy (Promega) for sequencing. For the *GFP* fusion construct, a BamHI site was introduced into *UGT89C1:UGT89C1* clone by PCR 3′ of the *ATG* (N-terminal fusion). PCR was performed with the primers *F7RT_R4_NGFP* 5′-GGATCCCATGATTG-ATGTTTTTTTCTTTC-3′ and *F7RT_F6_NGFP* 5′-GGATC-CACAACAACAACAACGAAGAAGC-3′. A previously produced *GFP* construct flanked by BamHI sites (46) was cloned into this BamHI site, resulting in *UGT89C1:GFP-UGT89C1*. This construct was cloned into the binary vector *pBART* (47) by NotI.

The molecular markers for the *rol1-2* and *fls1-3* mutations are described elsewhere (43, 44). For detection of *ugt89c1-3*, a PCR was performed using the primers *F7RT_F4* 5′-TGATG-CTTTCTCTATTAAGTCCAT-3′ and *F7RT_R5_CGFP* 5′-GGATCCCAAACACATCTCTGCAACGAG-3′. The PCR product was cut by ApaI (cuts wild type) and run on a 1.5% agarose gel. For detection of *ugt89c1-11*, PCR was performed using the primers *F7RT_F4* 5′-TGATGCTTTCTCTATTAA-GTCCAT-3′ and *F7RT_R5_CGFP* 5′-GGATCCCAAACACA-TCTCTGCAACGAG-3′. PCR was performed at 55 °C annealing temperature, 1.5 mM MgCl$_2$, and 1 min of elongation time, with 35 cycles. The PCR product was cut by BglII (cuts mutant) and run on a 1.5% agarose gel. All other *ugt89c1* alleles were confirmed by sequencing.

Microscopic Analysis—Phenotypic screening for and analysis of *ugt89c1 rol1-2* was performed using a binocular microscope. GFP fluorescence was photographed using a Leica DM6000 stereomicroscope. Gel prints of epidermal cells were produced following an established protocol (48) and observed by differential interference contrast microscopy using a Leica DMR microscope.

Flavonol Content Analysis—The analysis of the flavonol accumulation profile was done as described (44). Seedlings were grown in a vertical orientation for 6 days as described. One hundred intact seedlings were cut in the hypocotyl region, and roots and shoots were pooled separately, frozen in liquid nitrogen, and lyophilized to determine the dry weight. The dried material was incubated in 500 μl of 80% methanol overnight at 4 °C and subsequently macerated with a pestle, followed by vigorous vortexing. After pelleting the cell debris by centrifugation, the supernatant was transferred to a fresh tube and evaporated in a SpeedVac centrifuge, with the temperature being limited to a maximum of 42 °C. After evaporation, the pellet was resuspended in 100 μl of fresh 80% methanol and used for analysis. HPLC-ESI-MS and MS/MS experiments were performed on an ACQUITY UPLC (Waters) connected to a Bruker maXis high-resolution quadrupole time-of-flight mass spectrometer (Bruker Daltonics). An ACQUITY BEH C18 HPLC column (1.7 μm, 2.1 × 100 mm fitted with a 2 × 2-mm guard column) was used with a gradient of solvent A (H$_2$O, 0.1% (v/v) HCOOH) and solvent B (CH$_3$CN, 0.1% (v/v) HCOOH), at 0.45-ml flow rate and with a linear gradient from 5 to 95% B within 30 min.

The mass spectrometer was operated in the negative electrospray ionization mode. MS acquisitions were performed in the full scan mode in the mass range from m/z 50 to 2,000 at 25,000 resolution (full width at half-maximum) and two scans per second. The MS instrument was optimized for maximum signal intensities of quercitrine at m/z 447. Masses were calibrated with a 2 mM solution of sodium formate between m/z 180 and 1,472 prior to analysis. The lock mass signal of hexakis (1*H*,1*H*,2*H*-perfluoroethoxy)phosphazene at m/z 556.00195 was further used as lock mass during the HPLC run. Flavonols were identified by the molecular mass determined by MS and by interpretation of fragments obtained by MS/MS, by comparison of both fragmentation patterns and retention times with previous analyses (30), and by their absence in flavonol-less *rol1-2 fls1-3* mutants (44). Purification of each flavonol glycoside in sufficient quantities for producing standard curves was not possible. Therefore, the content of each individual flavonol was expressed as the peak area of the corresponding high-resolution extracted ion chromatogram. The total flavonol content was calculated by summing up all flavonol peak areas, divided by the weight of plant material used for extraction. Either the total or the individual flavonol contents were compared between different experiments.

Auxin Transport Experiments and Quantification of Derivatives—*Arabidopsis* mesophyll protoplasts were prepared as described (49) from rosette leaves of plants grown on soil under 100 μM m^{-2} s^{-1} white light, 8-h light, 16-h dark cycle at 22 °C. Intact protoplasts were isolated as described (50) and loaded by incubation with 1-[4-^{3}H]naphthalene acetic acid (25 Ci mmol^{-1}; American Radiolabeled Chemicals) on ice. External radioactivity was removed by separating protoplasts using a 50−30-5% Percoll gradient. Samples were incubated at 25 °C, and efflux was halted by silicon oil centrifugation. Effluxed radioactivity was determined by scintillation counting of aqueous phases and is presented as the relative efflux of the initial efflux (efflux prior to incubation), which was set to zero. Efflux experiments were performed with 3–5 independent protoplast preparations with four replicas for each time point. Basipetal (shoot-ward) auxin transport was measured according to Ref. 51. Radioactive auxin ([^{3}H]IAA) was applied to the root tips of 15 seedlings ($n = 4$), and 5–10-mm segments were cut after 18 h and counted. Segments in the wild-type Col were set as 100%, and others were calculated accordingly.

Measuring the concentration of auxin, auxin conjugates, and auxin degradation products was done as follows. The determination of IAA and its metabolites included extraction and purification (according to Ref. 52) followed by quantitation using LC-MS/MS (as described in Ref. 53). Briefly, a sample (about 100 mg of fresh weight) was homogenized in liquid nitrogen. The homogenate was supplied with 500 μl of cold extraction buffer (methanol/water/formic acid, 15/10/5, v/v/v, −20 °C) and with a mixture of stable isotope-labeled internal standards: [^{13}C$_6$]IAA (Cambridge Isotope Laboratories) and

$[^2H_5\text{-}^{15}N_1]$IAA-Asp, $[^2H_5\text{-}^{15}N_1]$IAA-Glu, and $[^2H_2]$OxIAA (OlChemIm, Olomouc, Czech Republic); 10 pmol each. After incubation for 30 min at $-20\,°C$, the extract was centrifuged at $28,000 \times g$ (centrifuge Eppendorf 5430 R, Eppendorf AG, Hamburg, Germany), and pellet was re-extracted once. Pooled supernatants were evaporated in vacuum concentrator (Alpha RVC, Martin Christ, Osterode am Harz, Germany), and then a sample residue was dissolved into 0.1 M formic acid and applied to mixed mode reversed phase-cation exchange SPE column (Oasis-MCX, Waters). Auxin and its metabolites were eluted with methanol. Eluate was evaporated to dryness in a vacuum concentrator and dissolved into 30 μl of 15% acetonitrile. An aliquot was analyzed on an HPLC (Ultimate 3000, Dionex) coupled to a hybrid triple quadrupole/linear ion trap mass spectrometer (3200 Q TRAP, Applied Biosystems) set in selected reaction monitoring mode. Quantification of hormones was done using the isotope dilution method with multilevel calibration curves ($r^2 > 0.99$). Data processing was carried out with Analyst 1.5 software (Applied Biosystems).

Accession Numbers—Sequence data from this article can be found in the Arabidopsis Genome Initiative or GenBank[TM]/ European Molecular Biology Laboratory (EMBL) databases under the following accession numbers: *FLS1*, At5g08640; *ROL1/RHM1*, At1g78570; *UGT89C1*, At1g06000.

Results

Altered Flavonol Glycosylation Suppresses the rol1-2 Shoot Growth Defect—The *rol1-2* shoot phenotype is characterized by hyponastic cotyledons, brick-shaped adaxial pavement cells of cotyledons, and deformed trichomes (Fig. 2A). Mutations in a glycosyltransferase involved in producing the *rol1-2* phenotype-inducing flavonol(s) would be expected to revert the *rol1-2* phenotype and act as suppressor(s) of the *rol1-2* phenotype. Thus, to identify possible *rol1-2* phenotype-inducing flavonols, *rol1-2* seeds were mutagenized with ethyl methanesulfonate. After mutagenesis, the seeds were propagated, and seedlings of the M2 generation were screened for a wild-type shoot phenotype that is characterized by epinastic cotyledons with puzzle-shaped pavement cells and upright, branched trichomes (Fig. 2A). The identified lines were propagated and confirmed in the M3 generation. Positive lines were backcrossed with *rol1-2*, and only those with an F2 segregation pattern indicating recessive suppressor mutations were further analyzed. Several lines were identified that suppressed the *rol1-2* phenotype, yet showed accumulation of flavonols to levels comparable with the wild type. Among these lines, only one group exhibited the lack of one specific type of flavonols, namely those rhamnosylated at the C7 position. Based on this finding, the previously identified flavonol 7-rhamnosyltransferase gene *UGT89C1* (29) was identified as a potential candidate suppressor gene, and sequencing of the *UGT89C1* locus At1g06000 indeed led to the identification of a mutation in this gene in all these mutants. In total, nine different *ugt89c1*-alleles were identified. Because two T-DNA insertion alleles of *ugt89c1* were already described, the newly identified EMS alleles were numbered *ugt89c1-3* to *ugt89c1-11*. In total, six missense and three nonsense mutations were identified (Table 1). The *ugt89c1-3* and *ugt89c1-6* alleles are affected in the same
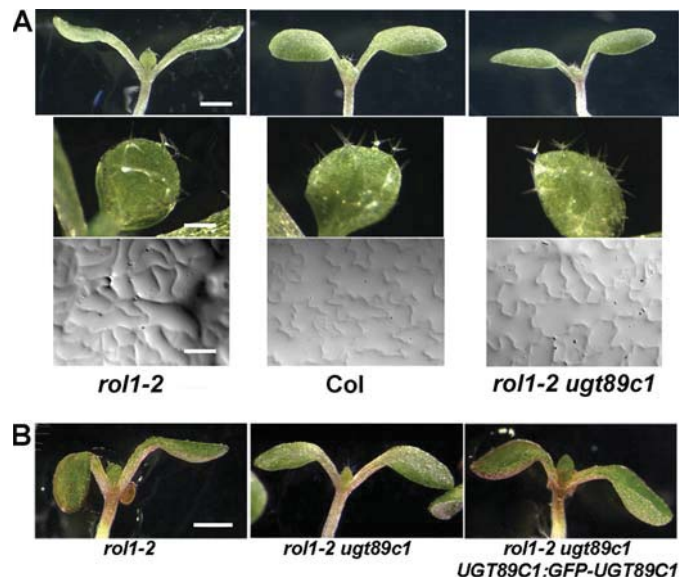

FIGURE 2. **The *rol1-2* mutant shoot cell growth phenotype is suppressed by mutations in *UGT89C1*.** *A*, the *rol1-2* mutant shows hyponastic bending of cotyledons, distorted trichomes, and brick-shaped adaxial pavement cells, whereas the wild type (*Col*) shows epinastic bending of cotyledons, normal shaped trichomes, and a jigsaw puzzle-like structure of adaxial pavement cells. All *ugt89c1* alleles identified in this study suppress the *rol1-2* shoot phenotype, *i.e. rol1-2 ugt89c1* double mutants develop comparable with the wild type. Pictures of the *rol1-2 ugt89c1-3* line are shown that are representative for all other *ugt89c1* lines. *B*, the *UGT89C1:GFP-UGT89C1* construct complements the *ugt89c1* mutation, and hence encodes a functional UGT89C1 protein, resulting in a *rol1-2* mutant phenotype. *Bars* = 1 mm for shoot (*A*, *upper panels*, and *B*); 0.2 mm for trichomes (*A*, *middle panels*); and 40 μm for pavement cells (*A*, *lower panels*).

codon, but the resulting nonsense mutations originate from two different mutation events. Hence, the *ugt89c1-3* and *ugt89c1-6* lines represent two independent alleles with the same effect at the protein level. All mutant *ugt89c1* alleles identified in this study lead to a comparable suppression of the *rol1-2* shoot phenotype, resulting in seedlings with epinastic cotyledons, jigsaw puzzle-shaped pavement cells, and wild type-like trichomes (Fig. 2A).

ugt89c1 Mutants Specifically Lack 7-Rhamnosylated Flavonols—A detailed analysis of the flavonol content of *rol1-2 ugt89c1* mutants was performed by HPLC-MS. Individual flavonols were identified by comparing the data with previous studies where flavonols were identified by HPLC-MS/MS, correlation with reference compounds, and the absence in a flavonol-deficient *flavonol synthase1* (*fls1*) mutant background (30, 44). For these and all subsequent analyses, the *ugt89c1-3* nonsense allele was used. The quantification of flavonol accumulation using the sum of areas of all identified flavonol-peaks in HPLC-MS analyses confirmed that the overall flavonol content of the *rol1-2 ugt89c1-3* line is comparable with the wild type or the *rol1-2* mutant (Fig. 3A). As a negative control, the *rol1-2 fls1-3* double mutant was included that shows a strongly reduced flavonol content due to a lesion in the *flavonol synthase 1* gene (44). The quantification of individual flavonol peaks confirmed the absence of all identifiable 7-*O*-rhamnosylated flavonols in *rol1-2 ugt89c1* mutants. Other flavonol glycoside derivatives were still present, some at levels higher than in the wild type or *rol1-2* single mutant, as shown for the kaempferol-3-*O*-glucoside (Fig. 3B). Flavonols of root and shoot tissue are

TABLE 1

List of *ugt89c1* alleles identified in this screen

Allele name	Mutation
ugt89c1-3	Stop 314[a]
ugt89c1-4	G123R
ugt89c1-5	S19F
ugt89c1-6	Stop 314[a]
ugt89c1-7	G249V
ugt89c1-8	Stop335
ugt89c1-9	D356N
ugt89c1-10	T4I
ugt89c1-11	R253W

[a] The mutations producing the stop codon are not identical.

affected, confirming the ubiquitous importance of UGT89C1 for flavonol 7-*O*-rhamnosylation. These data indicate a lack of genetic redundancy in *Arabidopsis* with respect to 7-*O*-rhamnosylation of flavonols. Hence, UGT89C1 appears to be the only enzyme that is capable of catalyzing this reaction to a significant extent. The lack of 7-*O*-rhamnosylated flavonols in *rol1-2 ugt89c1-3* suggests an important role of these compounds in the induction of the *rol1-2* shoot phenotype.

Different Protein Domains Are Affected in the ugt89c1 Alleles—Analysis of the UGT89C1 protein sequence was chosen as a strategy to elucidate the effect of the different mutations on the secondary and tertiary protein structure. UGT89C1 was compared with the flavonol-specific UGTs *Vv*GT1 from *Vitis vinifera* and *Mt*71G1 of *Medicago truncatula* whose secondary and tertiary structures are known (54, 55). *Vv*GT1 and *Mt*71G1 accept flavonols as donor substrates and therefore were selected for sequence and structural comparison. Previous analysis of four plant UDP-dependent glycosyltransferases revealed a low overall conservation on the protein sequence level, but a high conservation on the level of secondary and tertiary protein structure (56). The alignment (Fig. 4) shows only one short region of 45 amino acids, the PSPG domain that is relatively well conserved and important for binding of the UDP-sugar substrate. All three nonsense alleles and the missense allele *ugt89c1-9*, introducing an D356N substitution, affect residues in this PSPG domain. Mutational analysis has shown that the Asp residue affected in *ugt89c1-9* is essential for function of *Vv*GT1 (55). Of the remaining five alleles, four alter the N1- or C1-loops (*ugt89c1-5*, *-10*, and *ugt89c1-7*, *-11*, respectively) that are involved in forming the sugar donor binding pocket (56). Altogether, protein sequence analysis revealed that a vast majority of mutations that revert the *rol1-2* phenotype are directly related to sugar donor binding on the UGT89C1 enzyme.

UGT89C1 Expression Profile—The *rol1-2* cell growth phenotype in cotyledons is characterized by brick-shaped pavement cells on the adaxial side. Previous studies revealed that the flavonol synthase *FLS1* is expressed asymmetrically on the adaxial side (44), providing an explanation for the limitation of the flavonol-related cell growth defect to this side of the cotyledons. To investigate the localization of UGT89C1, a *GFP-UGT89C1* construct under the control of the *UGT89C1* promoter was produced and transformed into *Arabidopsis*. Complementation of the *rol1-2 ugt89c1-3* mutant was used to assess the impact of GFP on UGT89C1 protein activity. In the T2 generation, transgenic plants developed the typical *rol1-2* shoot growth phenotype (Fig. 2*B*), confirming complementation and
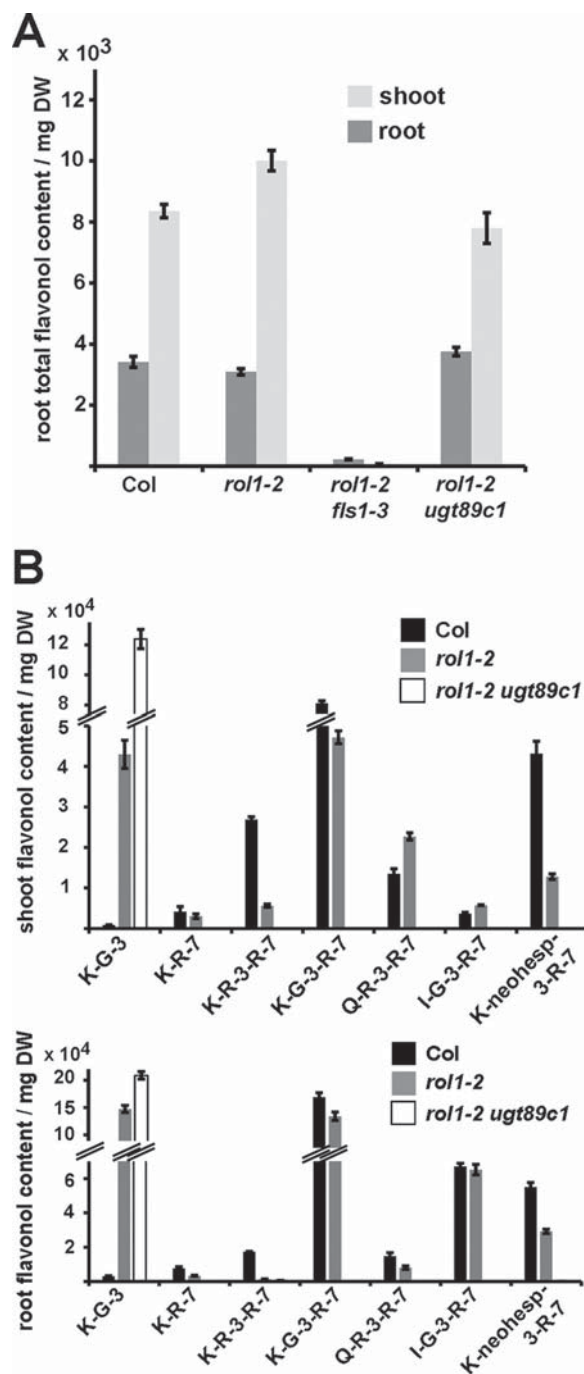
FIGURE 3. **Content of total flavonols and of 7-*O*-rhamnosylated flavonols.** *A*, total flavonol accumulation is comparable in the wild type, *rol1-2*, and *rol1-2 ugt89c1-3*. Values of *rol1-2 fls1-3*, which fail to accumulate flavonols, serve as negative control. *DW*, dry weight. *B*, the *rol1-2 ugt89c1-3* line shows a loss of 7-rhamnosylated flavonols, whereas *e.g.* 3-*O*-glucosylated flavonols are still present and accumulate both in the shoot (*upper graph*) and in the root (*lower graph*). Only a sub-selection of flavonols is shown. For quantification, the area under each peak of the HPLC elution profile was used as an arbitrary unit. *K-G-3*, kaempferol-3-*O*-glucoside; *K-R-7*, kaempferol-7-*O*-rhamnoside; *K-G-3-R-7*, kaempferol-3-*O*-glucoside-7-*O*-rhamnoside; *Q-R-3-R-7*, quercetin-3-*O*-7-*O*-rhamnoside; *I-G-3-R-7*, isorhamnetin-3-*O*-glucoside-7-*O*-rhamnoside; *K-neoh-3-R-7*, kaempferol-3-*O*-neohesperidoside-7-*O*-rhamnoside. *Error bars* indicate mean ± S.E.

thus activity of the GPF-UGT89C1 fusion protein. To assess protein localization, the *UGT89C1:GFP-UGT89C1* construct was transformed into wild-type *Arabidopsis* and GFP fluores-

```
                Nβ1    loopN1      Nα1              Nβ2   loopN2  Nα2
Vv GT1    --MSQTTTNPHVAVLAFPFSTHAAPLLAVVRRLAAAAPHAVFSFFFSTSQ---SNASIFHD
Mt 71G1   MSMSDINKNSELIFIPAPGIGHLASALEFAKLLTNHDKNLYITVFCIKFPGMPFADSYIK
UGT89C1   -MTTTTTTKKPHVLVIPFPQSGHMVPHLDLTHQILLRGATVTVLV--TP-----KNSSYLD
          :  ..: .: .:  *   *   *   ..: :          . .      . : .
              ugt89c1-10          ugt89c1-5
```

```
                  Nβ3      loopN3            Nα3
Vv GT1    SMHTMQ------CNIKSYDISDGVPEGYVFA-GRPQEDIELFTRAAPESFRQGMVMAVAE
Mt 71G1   SVLASQP------QIQLIDLPEVEPPPQELL-KSPEFYILTFLESLIPHVKATI---KTI
UGT89C1   ALRSLHSPEHFKTLILPFFPSHPCIPSGVESLQQLPLEAIVH-----------MFDALSR
          :: : :          *          *          *   *             :     :
```
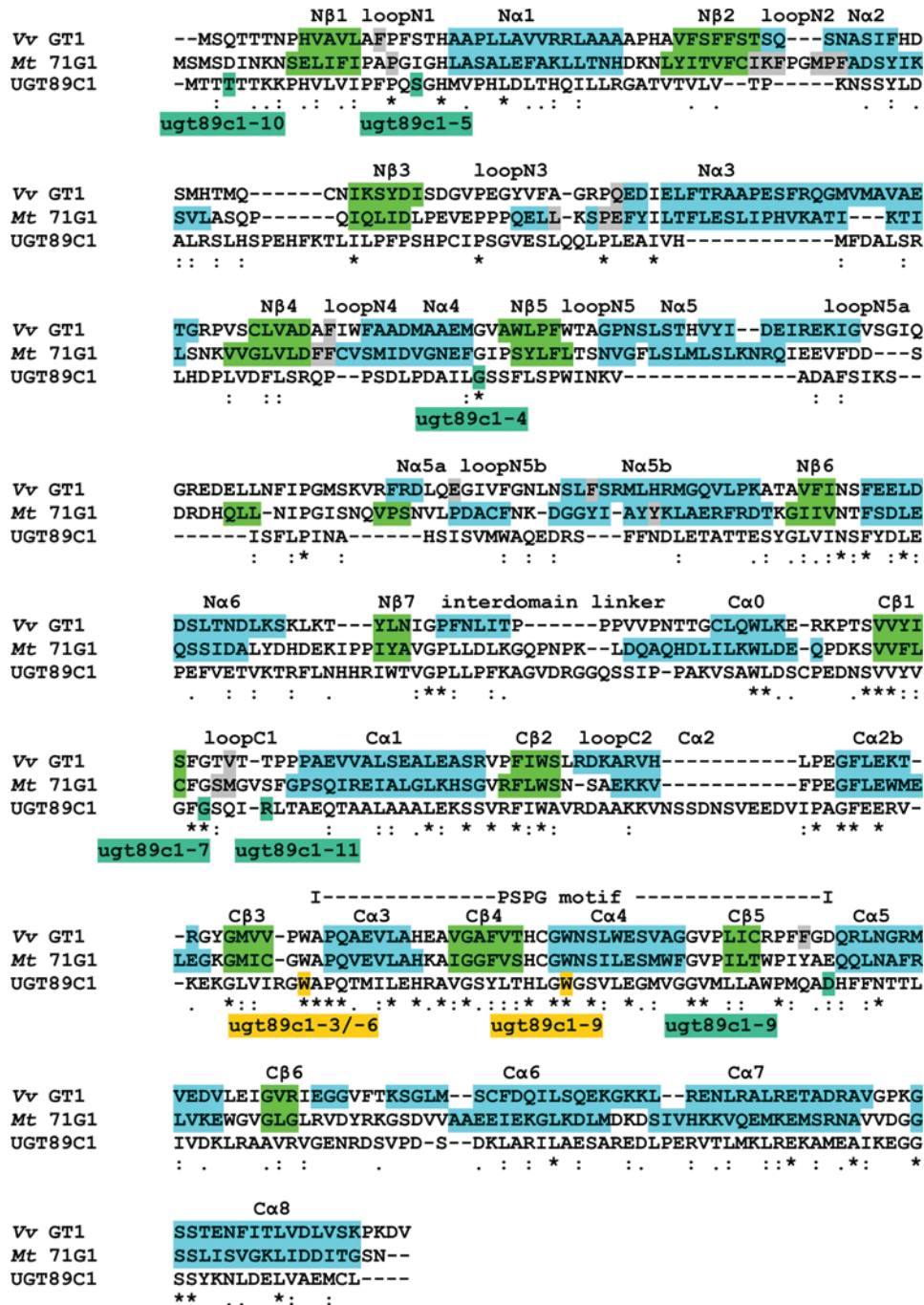
```
             Nβ4   loopN4  Nα4     Nβ5  loopN5  Nα5            loopN5a
Vv GT1    TGRPVSCLVADAFIWFAADMAAEMGVAWLPFWTAGPNSLSTHVYI--DEIREKIGVSGIQ
Mt 71G1   LSNKVVGLVLDFFCVSMIDVGNEFGIPSYLFLTSNVGFLSLMLSLKNRQIEEVFDD---S
UGT89C1   LHDPLVDFLSRQP--PSDLPDAILGSSFLSPWINKV--------------ADAFSIKS--
          :  ::      :   .  *                 :*                 : :
                    ugt89c1-4
```

```
                    Nα5a loopN5b      Nα5b            Nβ6
Vv GT1    GREDELLNFIPGMSKVRFRDLQEGIVFGNLNSLFSRMLHRMGQVLPKATAVFINSFEELD
Mt 71G1   DRDHQLL-NIPGISNQVPSNVLPDACFNK-DGGYI-AYYKLAERFRDTKGIIVNTFSDLE
UGT89C1   ------ISFLPINA------HSISVMWAQEDRS---FFNDLETATTESYGLVINSFYDLE
          :    :*  :         : :  :         :      .: .:.:*:* :*:
```

```
                  Nα6        Nβ7    interdomain linker     Cα0         Cβ1
Vv GT1    DSLTNDLKSKLKT---YLNIGPFNLITP------PPVVPNTTGCLQWLKE-RKPTSVVYI
Mt 71G1   QSSIDALYDHDEKIPPIYAVGPLLDLKGQPNPK--LDQAQHDLILKWLDE-QPDKSVVFL
UGT89C1   PEFVETVKTRFLNHHRIWTVGPLLPFKAGVDRGGQSSIP-PAKVSAWLDSCPEDNSVVYV
          . : :: . . .         :**: :.               **..   .***::
```

```
             loopC1       Cα1          Cβ2  loopC2   Cα2          Cα2b
Vv GT1    SFGTVT-TPPPAEVVALSEALEASRVPFIWSLRDKARVH-----------LPEGFLEKT-
Mt 71G1   CFGSMGVSFGPSQIREIALGLKHSGVRFLWSN-SAEKKV-----------FPEGFLEWME
UGT89C1   GFGSQI-RLTAEQTAALAAALEKSSVRFIWAVRDAAKKVNSSDNSVEEDVIPAGFEERV-
          **:        :    :: .*: * * *:*.       :            :* ** *
             ugt89c1-7       ugt89c1-11
```

```
                 I--------------PSPG motif --------------I
             Cβ3         Cα3      Cβ4         Cα4         Cβ5         Cα5
Vv GT1    -RGYGMVV-PWAPQAEVLAHEAVGAFVTHCGWNSLWESVAGGVPLICRPFFGDQRLNGRM
Mt 71G1   LEGKGMIC-GWAPQVEVLAHKAIGGFVSHCGWNSILESMWFGVPILTWPIYAEQQLNAFR
UGT89C1   -KEKGLVIRGWAPQTMILEHRAVGSYLTHLGWGSVLEGMVGGVMLLAWPMQADHFFNTTL
          *:.  *****. :  ** *.*:*:**  *: *:    **  : ** .  .::  :*
             ugt89c1-3/-6          ugt89c1-9    ugt89c1-9
```

```
                 Cβ6        Cα6              Cα7
Vv GT1    VEDVLEIGVRIEGGVFTKSGLM--SCFDQILSQEKGKKL--RENLRALRETADRAVGPKV
Mt 71G1   LVKEWGVGLGLRVDYRKGSDVVAAEEIEKGLKDLMDKDSIVHKKVQEMKEMSRNAVVDGG
UGT89C1   IVDKLRAAVRVGENRDSVPD-S--DKLARILAESAREDLPERVTLMKLREKAMEAIKEGG
          :.    .: .:           . :.: *  :.    : .:    ::* : .*:   *
```

```
                 Cα8
Vv GT1    SSTENFITLVDLVSKPKDV
Mt 71G1   SSLISVGKLIDDITGSN--
UGT89C1   SSYKNLDELVAEMCL----
          **  .. *: :
```

FIGURE 4. **Structural alignment of primary sequences of different UGTs with UGT89C1.** The crystal structure of VvGT1 (*V. vinifera* (*Vv*)) and Mt71G1 (*Medicago truncatula* (*Mt*)) was already solved, and different domains were marked with colors. α-Helices are highlighted in *blue*, and β-strands are in *light green*. The structurally important loops are labeled. Nonsense mutations identified in this screen are marked in *beige*, and missense mutations are in *dark green*. The *dashed line* indicates the PSPG motif important for UDP-sugar donor specificity. Residues reported to be involved in acceptor pocket formation are highlighted in *gray*. *Asterisks* mark identity, *colons* mark high similarities, *single dots* mark lower similarities, and *blank positions* indicate no similarities between the amino acids in the compared sequences. Adopted from Ref. 56.

cence was analyzed in seedlings of the T2 generation of several independent transgenic lines. GFP fluorescence could be detected on the adaxial side of cotyledons and emerging leaves (Fig. 5A, C), comparable with the previously reported pattern observed in *FLS1:GFP-FLS1* (Fig. 5B) and *RHM1:RHM1-GFP* (*RHM1* is identical to *ROL1*) transgenic lines (44). Trichomes also showed a strong GFP fluorescence (Fig. 5G). In roots, GFP fluorescence was predominant in columella cells and in the late elongation/early differentiation zone, correlating with zones of

high auxin concentrations. Subcellularly, GFP-UGT89C1 localizes to the cytoplasm and the nucleus (Fig. 5, D–F). The expression pattern of *GFP-UGT89C1* is similar to *FLS1* (44) confirming the previous finding that *UGT89C1* is co-expressed with other genes coding for enzymes of the flavonoid biosynthesis pathway (29).

Auxin Distribution but Not Auxin Transport Is Modified by the ugt89c1 Mutations—Flavonols have been shown to modify auxin-related processes (13, 14). *rol1-2* mutant seedlings
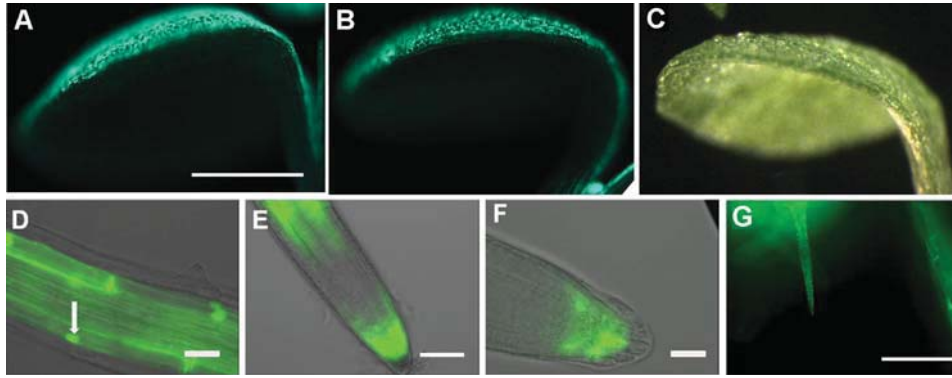
FIGURE 5. **Localization of GFP-UGT89C1.** *A* and *B*, in cotyledon of 6-day-old seedlings, fluorescence induced by *UGT89C1:GFP-UGT89C1* (A) is restricted to the adaxial side, very similar to seedlings containing *FLS1:FLS1-GFP* (B). *C*, bright field image of a cotyledon corresponding to those shown in *A* and *B*. In roots, fluorescence of GFP-UGT89C1 was observed in the cortex and vascular cell layers of the differentiation zone. *D*, on the subcellular level, a fraction of the fusion protein localizes to the nucleus (*arrow*). *E*, in root tips, fluorescence occurred around the meristematic and later elongation zone. *F*, detailed analysis of root tips revealed *GFP-UGT89C1* expression in columella and lateral root cap cells. *G*, GFP-UGT89C1 induced fluorescence in trichomes. *Bars* = 1 mm (*A–C*); 15 μm (*D* and *F*); 30 μm (*E*); and 100 μm (*G*).

indeed show an altered auxin distribution and transport activity, as determined by auxin concentration measurements and transport assays (30, 44). To determine whether *ugt89c1* functions as a suppressor of *rol1-2* by influencing auxin distribution, auxin export was measured in the wild type, *rol1-2*, and *rol1-2 ugt89c1* mutant lines. Due to the strong growth defect of *rol1-2* mutant seedlings, which might interfere with interpretation of auxin transport in a whole-seedling assay, rosette leaf mesophyll protoplasts were used following an established protocol (44). In a first step, flavonols were extracted from wild-type, *rol1-2*, and *rol1-2 ugt89c1* protoplasts to confirm that the mutations have an effect on flavonol accumulation in this cell type. Comparable with flavonols of seedlings, flavonols of *rol1-2* protoplasts revealed a glycosylation profile that is distinct from wild-type protoplasts in that they accumulate fewer rhamnosylated and more glucosylated flavonols (Fig. 6*A*) (30). *rol1-2 ugt89c1* protoplasts did not accumulate 7-*O*-rhamnosylated flavonols. Hence, protoplasts of the different genotypes showed the expected flavonol glycosylation profile, making them suitable to investigate the effect of the two mutations on auxin transport. Auxin export rates were determined in protoplasts using the synthetic auxin, 1-NAA, and revealed that the *rol1-2* mutant shows a modified transport efficiency as compared with the wild type. *rol1-2 ugt89c1-3* double mutant protoplasts, however, show a transport rate that is not different from the one of *rol1-2* (Fig. 6*B*). Hence, mutations in *ugt89c1* suppress the *rol1-2* phenotype by an auxin transport-independent manner. This is particularly interesting because the flavonol-less *rol1-2 fls1* mutant suppresses *rol1-2* by changing auxin transport back to wild-type levels (44). Hence, the mode of action of *fls1* and *ugt89c1* is different. To sustain cellular auxin transport data and to back up measurements performed with synthetic auxin 1-NAA, we measured basipetal (shoot-ward) IAA transport in roots. Comparable with 1-NAA transport in protoplasts, root basipetal transport of IAA was revealed to be changed in *rol1-2* as compared with the wild type. The *rol1-2 ugt89c1* double mutant shows transport activity similar to *rol1-2*, again indicating that *ugt89c1* does not modify the *rol1-2*-induced alteration in auxin transport (Fig. 6*C*). To investigate whether *ugt89c1* changes auxin levels in a different way, con-

centrations of free auxin and auxin-related metabolites were determined in wild type, *rol1-2*, and *rol1-2 ugt89c1* mutant seedlings. Here, two additional lines were included: the *ugt89c1* single mutant to confirm effects found for *rol1-2 ugt89c1*; and the *rol1-2 fls1-3* double mutant to obtain indications of whether *ugt89c1* and *fls1-3* indeed suppress *rol1-2* by different means. The levels of the prevailing auxin of *Arabidopsis*, IAA, was subject to variation between several biologically independent experiments. As a consequence, the increase in auxin concentration in *rol1-2* as compared with the wild type was not as pronounced as reported previously (30) and did not fulfill the criteria of statistical significance (*t* test, $p < 0.05$). The reason for the observed variation is not clear at this point. Quantification of the auxin precursor indole-3-acetonitrile (IAN) and auxin conjugates and degradation products, on the other hand, gave very consistent results: *ugt89c1* shows increased accumulation of IAN as well as of auxin conjugates and degradation intermediates such as IAA-Glc or oxIAA-Glc (Fig. 7). This effect of *ugt89c1* is observed not only in the context of the *rol1-2* mutation that causes aberrant accumulation of flavonols, but also in the *ugt89c1* single mutant as compared with the wild type, suggesting that the accumulation of auxin precursor and derivatives is genuinely affected by flavonol glycosides.

Discussion

Flavonoids are a group of phenylpropanoic secondary metabolites known to influence cellular processes. They are of interest as nutrition additives due to their health-promoting effect (57). However, the knowledge of the effects of flavonoids on cellular processes in either animals or plants is still limited. The *Arabidopsis rol1-2* shoot phenotype, characterized by defects in cell growth and development, is induced by flavonols, a subgroup of flavonoids (30, 44), and thus represents a model to characterize the active flavonol(s) and their mode of action.

Flavonol Glycosides Influence Plant Development—The study presented here identifies 7-*O*-rhamnosylated flavonols as being important for inducing the growth defects in *rol1-2*. The enzyme UGT89C1, conjugating rhamnose onto flavonols (29), is encoded by a single gene in *Arabidopsis*, and mutations in *UGT89C1* were identified as suppressors of the *rol1-2* pheno-
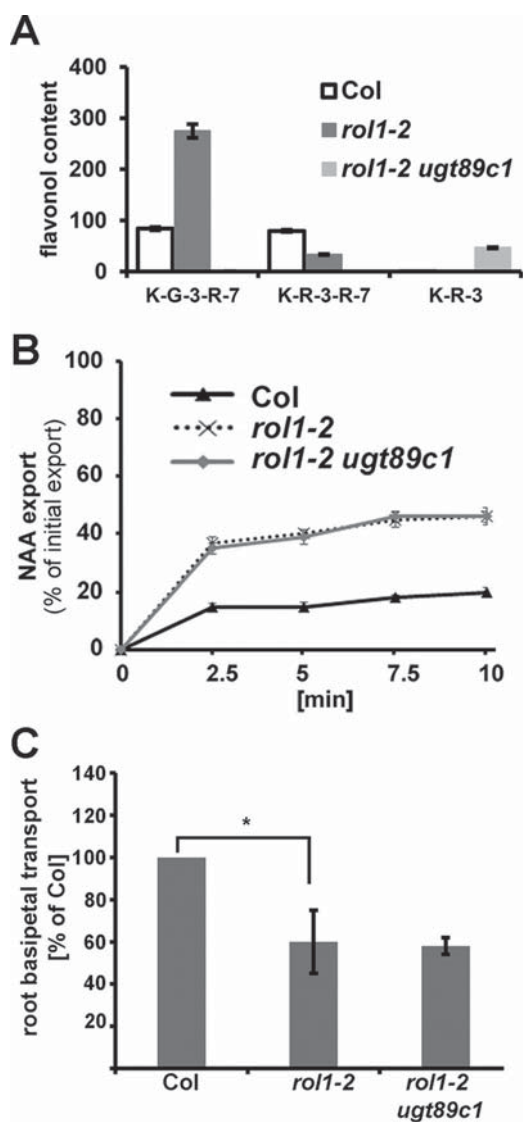
FIGURE 6. **Auxin transport in *rol1-2* plants is not affected by *ugt89c1*.** *A*, flavonol content analysis of protoplasts revealed the same effects of *rol1-2* and *ugt89c1* mutations as in intact plants. The area under each peak of the HPLC elution profile was used to determine flavonol content. *K-G-3-R-7*, kaempferol-3-*O*-glucoside-7-*O*-rhamnoside; *K-R-3*, kaempferol-3-*O*-rhamnoside. *B*, auxin (1-NAA) export from protoplasts is affected in *rol1-2* as compared with the wild type (*Col*) but not altered by the *ugt89c1* mutation. *C*, as compared with the wild type (*Col*), *rol1-2* and *rol1-2 ugt89c1* show similar, reduced basipetal IAA transport in roots. *Asterisks* indicate statistically significant differences (*t* test, $p < 0.05$). *Error bars* indicate mean ± S.E.

FIGURE 7. ***ugt89c1*** **affects levels of auxin precursor and metabolites.** Quantification of the auxin conjugates IAA-Glc and IAA-Glu, the auxin precursor IAN, and the degradation products oxIAA and oxIAA-Glc is shown for wild type (*Col*), *rol1-2*, and *ugt89c1* single mutants, and for *rol1-2 ugt89c1* and *rol1-2 fls1-3* double mutants. *FW*, fresh weight. Statistically significant differences (*t* test) with $p < 0.05$ and $p < 0.01$ are indicated with one and two asterisks, respectively. *Error bars* indicate mean ± S.E.

type. In seedling shoots, *UGT89C1* expression is limited to the adaxial side of cotyledons, emerging leaves, and trichomes. The same protein accumulation pattern has been found for ROL1/RHM1 and FLS1 (44), which explains the asymmetry in the flavonol-induced growth phenotype that is limited in cotyledons to the adaxial side. The co-localization is also in line with previous findings that genes involved in flavonoid biosynthesis (including *FLS1*, *RHM1*, and *UGT89C1*) are co-regulated (26). The data suggest that flavonol glycosides are the active flavonol species and that 7-*O*-rhamnosylated flavonols are involved in inducing the *rol1-2* phenotype. Evidence for an active role of glycosylated flavonols in plant development was also provided by the analysis of the 3-*O*-glucosyltransferase mutant *ugt78d2*, which shows a dwarfed growth phenotype. This mutant con-
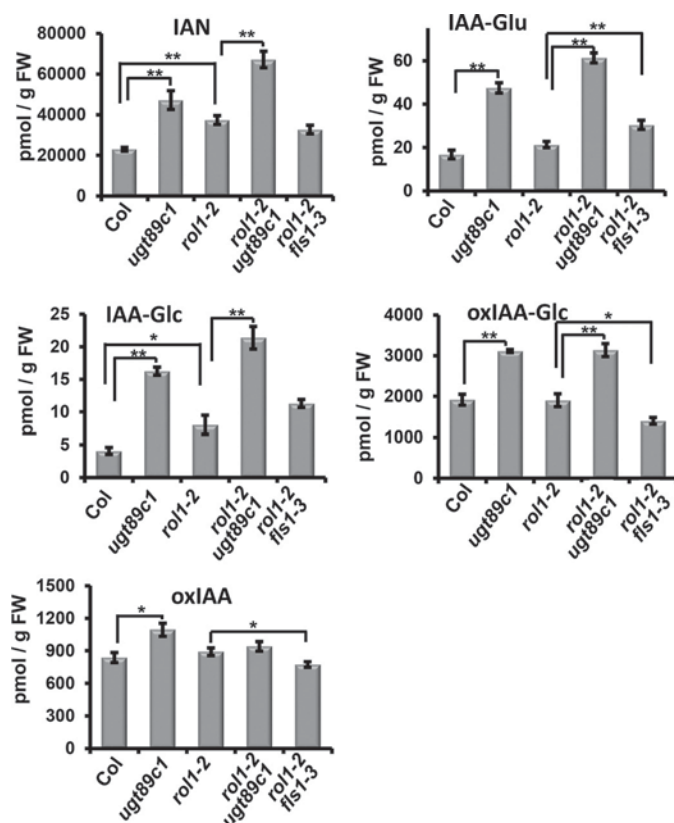
tains increased levels of 3-*O*-7-*O*-rhamnosylated flavonols, and mutating either the 3-*O*-rhamnosyltransferases or the 7-*O*-rhamnosyltransferases *ugt78d1* or *ugt89c1*, respectively, suppresses the dwarfed phenotype of *ugt78d2*. Hence, 3-*O*-7-*O*-rhamnosylated flavonols appear to induce the growth defects developed by the *ugt78d2* mutant (31). Both the *ugt78d2* and the *rol1-2* mutant phenotypes are also found in combination with the *tt7* mutation (30, 31) that prevents synthesis of quercetin and causes over-accumulation of kaempferol (Fig. 1). Thus, accumulation of the flavonol kaempferol appears to be sufficient to interfere with proper plant development. Similarly, the *tt7* single mutant was reported to have increased inhibition of auxin transport, again suggesting that kaempferol and its glycosylated forms are particularly active flavonols (13). The mechanism of flavonol-induced growth defects, however, is not the same in *rol1-2* and *ugt72d2*. First, in contrast to *ugt78d2*, there is a reduction of 3-*O*-7-*O*-rhamnosylated flavonols in *rol1-2* as compared with the wild type (30). Second, although introducing the *ugt89c1* mutation suppresses both *ugt78d2* and *rol1-2*, the introduction of the 3-*O*-rhamnosyl transferase mutation *ugt78d1* only suppresses *ugt72d2* but not *rol1-2* (30, 31). This raises the question as to how suppression of the *ugt78d2* and *rol1-2* mutant phenotypes is induced. Although the mechanism of suppression of the *ugt78d2* mutant by *ugt78d1* and *ugt89c1* has not yet been investigated (31), the

work presented here suggests that *ugt89c1* suppresses the *rol1-2* phenotype by modulating levels of the auxin precursor IAN and auxin metabolites rather than auxin transport.

Flavonols Influence Auxin Homeostasis in Several Ways— The suppression of *rol1-2* by *tt4*, *tt6*, and *fls1* (30, 44) fit the picture of flavonols being negative regulators of auxin transport (11). Indeed, interfering with flavonol biosynthesis in *rol1-2* by an *fls1* mutation reverts the modified auxin transport to wild-type levels and suppresses the *rol1-2* phenotype. In contrast to the *fls1* mutation, however, *ugt89c1* does not seem to interfere with auxin transport. As compared with the wild type, the *rol1-2* mutant shows an increase in auxin efflux in the protoplast assay but a decrease in auxin transport in the root basipetal transport. This discrepancy can be explained by the very different experimental setup in the assays. In the protoplast assay, primarily auxin efflux is measured from a non-polarized, cellular system after loading with radioactive auxin. In contrast, the root basipetal transport assay is performed on the entire root, so that the resulting value comes from the complex auxin transport machinery present in the root tissues. However, and importantly, the absence of any effect of the additional *ugt89c1* mutation is found in both systems. This unexpected finding can be explained by different flavonol species having different functions in terms of regulating auxin levels. Although some interfere with auxin transport, others seem to influence auxin metabolism. Kaempferols are important for the development of the *ugt78d2* and *rol1-2* phenotypes or for pollen development in maize (6, 30, 31), whereas other studies point at quercetin as an important flavonol (58, 59). In the *rol1-2 fls1* double mutant, all flavonols are absent, resulting in wild type-like auxin transport, whereas a defect in 7-*O*-rhamnosylation only interferes with auxin metabolism but not transport. An indication for multiple modes of action of flavonols was also obtained from analyzing the *rol1-2* shoot phenotype in more detail. In seedlings, a correlation between increased auxin levels and growth defects was observed. However, phenocopying the increased auxin levels in wild-type seedlings by exposing them to the auxin efflux inhibitor 1-naphthylphthalamic acid resulted in hyponastic cotyledons comparable with the *rol1-2* shoot phenotype, whereas the defects in pavement cell shape and trichome development were not observed (30). Hence, negatively regulating auxin transport is likely not the only way by which flavonols in the *rol1-2* mutant interfere with plant development. The results presented here suggest that UGT89C1 influences the activity of auxin biosynthesis and its conjugation/degradation. Although oxIAA and oxIAA-Glc are irreversible degradation intermediates, IAA-amino acid derivatives can mostly be converted back to active, free auxin (32–34, 60). Interfering with the activity of amidohydrolases that convert IAA-amino acid conjugates to free IAA affects free auxin levels and induces auxin-related phenotypes (61, 62). A mutation in *ugt89c1* causes an increase in the level of auxin precursor and auxin metabolites, the only exception being oxIAA accumulation in *rol1-2 ugt89c1* that is comparable with *rol1-2*. Both low-abundant (such as IAA-Glu or IAA-Glc) as well as highly abundant (such as the auxin precursor IAN or the auxin degradation product oxIAA-Glc) auxin derivatives are affected to a similar extent. However, the low-abundant IAA derivatives are

reversible conjugates that contribute to the pool of all IAA metabolites only very little (<1%). The accumulation of the precursor IAN in the *ugt89c1* and *ugt89c1 rol1-2* mutants suggests that conversion of this molecule to free IAA is inhibited. On the other hand, according to the levels of oxIAA-Glc, irreversible oxidative degradation is increased in those mutants. Thus, UGT89C1 seems to influence the production as well as the degradation of auxin. Considering the large amount of the precursor IAN in the entire pool of auxin-related metabolites, the regulation of the last step of auxin biosynthesis appears to be a main target process of the activity of UGT89C1. At this point, it is not clear why these changes in the pool of auxin and its derivatives are not reflected in a clear change in the level of free auxin. Several repetitions of auxin measurements gave somewhat varying results with an increase in *rol1-2* as compared with the wild type, whereas *rol1-2 ugt89c1* reduced auxin levels again. However, the differences were not severalfold, did not fulfill the criteria of statistical significance, and therefore cannot be considered in the interpretation. Such variations may reflect fine-tuning of levels of free auxin as the only auxin-active form in relation to subtle variations in developmental stages of plant material used to analyze auxin content in biologically independent samples. It can be assumed that the level of free auxin is under strict control and may be modified only temporarily and locally by control mechanisms that are functional in the absence of UGT89C1. Blocking flavonol biosynthesis in the *rol1-2 fls1-3* mutant has comparatively little effect on the auxin derivatives. In three out of five auxin-related compounds, the changes induced by *fls1-3* are the opposite of those induced by *ugt89c1*, *i.e.* oxIAA-Glc is reduced in *rol1-2 fls1-3* as compared with *rol1-2*, but increased in *rol1-2 ugt89c1*. These data indicate again that changes in the flavonol glycosylation pattern do not have the same effect on auxin levels as blocking altogether flavonol synthesis. Presumably, the balance between different glycosylated forms of flavonols including 7-*O*-rhamnosylated flavonols is critical for auxin homeostasis, and thus, for proper plant development. The mechanism by which flavonols influence auxin conjugation and catabolism remains to be uncovered. The level of oxIAA has been shown to be increased in the flavonol-deficient *tt4* mutant and reduced in the flavonol overaccumulator *tt3*, an observation that is attributed to the reactive oxygen species-scavenging activity of flavonols (9, 42). However, mutations in *ugt89c1* do not affect the overall accumulation of flavonols. This suggests that different flavonol glycosides might have different reactive oxygen species-scavenging activities, possibly because of distinct subcellular localization. Alternatively, *ugt89c1* mutations might not influence auxin oxidation via modulated reactive oxygen species-scavenging activity. It has been shown that changing flavonol glycosylation affects gene expression (8), and thereby, genes involved in auxin metabolism might also be affected. Formally, it cannot be excluded that UGT89C1 has another biochemical activity in addition to its function as a rhamnosyltransferase. However, UGT89C1 appears to recruit specifically Rha as the substrate and flavonols as acceptor for the glycosyltransferase reaction, and its gene expression is tightly linked with other genes involved in flavonol biosynthesis (26, 29), making such a scenario less likely.

9

Together, the findings of this study reveal the effect of flavonol glycosides on auxin metabolic turnover. In addition to the known effect of flavonols on auxin transport, this represents a new mechanism for flavonols to influence auxin homeostasis.

References

1. Lepiniec, L., Debeaujon, I., Routaboul, J. M., Baudry, A., Pourcel, L., Nesi, N., and Caboche, M. (2006) Genetics and biochemistry of seed flavonoids. *Annu. Rev. Plant Biol.* **57,** 405–430
2. Costa, D., Galvao, A. M., Di Paolo, R. E., Freitas, A. A., Lima, J. C., Quina, F. H., and Macanita, A. L. (2015) Photochemistry of the hemiketal form of anthocyanins and its potential role in plant protection from UV-B radiation. *Tetrahedron* **71,** 3157–3162
3. Zhang, J., Subramanian, S., Stacey, G., and Yu, O. (2009) Flavones and flavonols play distinct critical roles during nodulation of *Medicago truncatula* by *Sinorhizobium meliloti*. *Plant J.* **57,** 171–183
4. Brown, J. E., Khodr, H., Hider, R. C., and Rice-Evans, C. A. (1998) Structural dependence of flavonoid interactions with Cu^{2+} ions: implications for their antioxidant properties. *Biochem. J.* **330,** 1173–1178
5. Taylor, L. P., and Grotewold, E. (2005) Flavonoids as developmental regulators. *Curr. Opin. Plant Biol.* **8,** 317–323
6. Mo, Y. Y., Nagel, C., and Taylor, L. P. (1992) Biochemical complementation of chalcone synthase mutants defines a role for flavonols in functional pollen. *Proc. Natl. Acad. Sci. U.S.A.* **89,** 7213–7217
7. Peer, W. A., and Murphy, A. S. (2006) Flavonoids as signal molecules. in *The Science of Flavonoids* (Grotewold, E. ed), pp. 239–268, Springer-Verlag, Berlin
8. Yin, R., Messner, B., Faus-Kessler, T., Hoffmann, T., Schwab, W., Hajirezaei, M.-R., von Saint Paul, V., Heller, W., and Schäffner, A. R. (2012) Feedback inhibition of the general phenylpropanoid and flavonol biosynthetic pathways upon a compromised flavonol-3-*O*-glycosylation. *J. Exp. Bot.* **63,** 2465–2478
9. Nakabayashi, R., Yonekura-Sakakibara, K., Urano, K., Suzuki, M., Yamada, Y., Nishizawa, T., Matsuda, F., Kojima, M., Sakakibara, H., Shinozaki, K., Michael, A. J., Tohge, T., Yamazaki, M., and Saito, K. (2014) Enhancement of oxidative and drought tolerance in *Arabidopsis* by overaccumulation of antioxidant flavonoids. *Plant J.* **77,** 367–379
10. Jacobs, M., and Rubery, P. H. (1988) Naturally-occurring auxin transport regulators. *Science* **241,** 346–349
11. Buer, C. S., and Muday, G. K. (2004) The *transparent testa4* mutation prevents flavonoid synthesis and alters auxin transport and the response of *Arabidopsis* roots to gravity and light. *Plant Cell* **16,** 1191–1205
12. Brown, D. E., Rashotte, A. M., Murphy, A. S., Normanly, J., Tague, B. W., Peer, W. A., Taiz, L., and Muday, G. K. (2001) Flavonoids act as negative regulators of auxin transport *in vivo* in *Arabidopsis*. *Plant Physiol.* **126,** 524–535
13. Peer, W. A., Bandyopadhyay, A., Blakeslee, J. J., Makam, S. N., Chen, R. J., Masson, P. H., and Murphy, A. S. (2004) Variation in expression and protein localization of the PIN family of auxin efflux facilitator proteins in flavonoid mutants with altered auxin transport in *Arabidopsis thaliana*. *Plant Cell* **16,** 1898–1911
14. Peer, W. A., Blakeslee, J. J., Yang, H., and Murphy, A. S. (2011) Seven things we think we know about auxin transport. *Mol. Plant* **4,** 487–504
15. Zažímalová, E., Murphy, A. S., Yang, H., Hoyerová, K., and Hosek, P. (2010) Auxin transporters: why so many? *Cold Spring Harb. Perspect. Biol.* **2,** a001552
16. Remmer, J., and Murphy, A. S. (2014) Intercellular transport of auxin. in *Auxin and its role in plant development* (Zažímalová, E., Petrášek, J., and Benková, E. eds.), pp. 75–100, Springer, Vienna
17. Bouchard, R., Bailly, A., Blakeslee, J. J., Oehring, S. C., Vincenzetti, V., Lee, O. R., Paponov, I., Palme, K., Mancuso, S., Murphy, A. S., Schulz, B., and Geisler, M. (2006) Immunophilin-like TWISTED DWARF1 modulates auxin efflux activities of *Arabidopsis* P-glycoproteins. *J. Biol. Chem.* **281,** 30603–30612
18. Bailly, A., Sovero, V., Vincenzetti, V., Santelia, D., Bartnik, D., Koenig, B. W., Mancuso, S., Martinoia, E., and Geisler, M. (2008) Modulation of P-glycoproteins by auxin transport inhibitors is mediated by interaction with immunophilins. *J. Biol. Chem.* **283,** 21817–21826
19. Michniewicz, M., Zago, M. K., Abas, L., Weijers, D., Schweighofer, A., Meskiene, I., Heisler, M. G., Ohno, C., Zhang, J., Huang, F., Schwab, R., Weigel, D., Meyerowitz, E. M., Luschnig, C., Offringa, R., and Friml, J. (2007) Antagonistic regulation of PIN phosphorylation by PP2A and PINOID directs auxin flux. *Cell* **130,** 1044–1056
20. Henrichs, S., Wang, B., Fukao, Y., Zhu, J., Charrier, L., Bailly, A., Oehring, S. C., Linnert, M., Weiwad, M., Endler, A., Nanni, P., Pollmann, S., Mancuso, S., Schulz, A., and Geisler, M. (2012) Regulation of ABCB1/PGP1-catalysed auxin transport by linker phosphorylation. *EMBO J.* **31,** 2965–2980
21. Chen, R., Hilson, P., Sedbrook, J., Rosen, E., Caspar, T., and Masson, P. H. (1998) The *Arabidopsis thaliana AGRAVITROPIC* 1 gene encodes a component of the polar-auxin-transport efflux carrier. *Proc. Natl. Acad. Sci. U.S.A.* **95,** 15112–15117
22. Luschnig, C., Gaxiola, R. A., Grisafi, P., and Fink, G. R. (1998) EIR1, a root-specific protein involved in auxin transport, is required for gravitropism in *Arabidopsis thaliana*. *Genes Dev.* **12,** 2175–2187
23. Santelia, D., Henrichs, S., Vincenzetti, V., Sauer, M., Bigler, L., Klein, M., Bailly, A., Lee, Y., Friml, J., Geisler, M., and Martinoia, E. (2008) Flavonoids redirect PIN-mediated polar auxin fluxes during root gravitropic responses. *J. Biol. Chem.* **283,** 31218–31226
24. Koornneef, M. (1990) Mutations affecting the testa color in *Arabidopsis*. *Arab. Inf. Serv.* **19,** 113–115
25. Routaboul, J. M., Kerhoas, L., Debeaujon, I., Pourcel, L., Caboche, M., Einhorn, J., and Lepiniec, L. (2006) Flavonoid diversity and biosynthesis in seed of *Arabidopsis thaliana*. *Planta* **224,** 96–107
26. Yonekura-Sakakibara, K., Tohge, T., Matsuda, F., Nakabayashi, R., Takayama, H., Niida, R., Watanabe-Takahashi, A., Inoue, E., and Saito, K. (2008) Comprehensive flavonol profiling and transcriptome coexpression analysis leading to decoding gene-metabolite correlations in *Arabidopsis*. *Plant Cell* **20,** 2160–2176
27. Jones, P., Messner, B., Nakajima, J., Schäffner, A. R., and Saito, K. (2003) UGT73C6 and UGT78D1, glycosyltransferases involved in flavonol glycoside biosynthesis in *Arabidopsis thaliana*. *J. Biol. Chem.* **278,** 43910–43918
28. Tohge, T., Nishiyama, Y., Hirai, M. Y., Yano, M., Nakajima, J., Awazuhara, M., Inoue, E., Takahashi, H., Goodenowe, D. B., Kitayama, M., Noji, M., Yamazaki, M., and Saito, K. (2005) Functional genomics by integrated analysis of metabolome and transcriptome of *Arabidopsis* plants overexpressing an MYB transcription factor. *Plant J.* **42,** 218–235
29. Yonekura-Sakakibara, K., Tohge, T., Niida, R., and Saito, K. (2007) Identification of a flavonol 7-*O*-rhamnosyltransferase gene determining flavonol pattern in *Arabidopsis* by transcriptome coexpression analysis and reverse genetics. *J. Biol. Chem.* **282,** 14932–14941
30. Ringli, C., Bigler, L., Kuhn, B. M., Leiber, R. M., Diet, A., Santelia, D., Frey, B., Pollmann, S., and Klein, M. (2008) The modified flavonol glycosylation profile in the *Arabidopsis rol1* mutants results in alterations in plant growth and cell shape formation. *Plant Cell* **20,** 1470–1481
31. Yin, R., Han, K., Heller, W., Albert, A., Dobrev, P. I., Zažímalová, E., and Schäffner, A. R. (2014) Kaempferol 3-*O*-rhamnoside-7-*O*-rhamnoside is an endogenous flavonol inhibitor of polar auxin transport in *Arabidopsis* shoots. *New Phytol.* **201,** 466–475
32. Ostin, A., Kowalyczk, M., Bhalerao, R. P., and Sandberg, G. (1998) Metabolism of indole-3-acetic acid in *Arabidopsis*. *Plant Physiol.* **118,** 285–296
33. Tam, Y. Y., Epstein, E., and Normanly, J. (2000) Characterization of auxin conjugates in *Arabidopsis*: low steady-state levels of indole-9-acetyl-aspartate indole-3-acetyl-glutamate, and indole-3-acetyl-glucose. *Plant Physiol.* **123,** 589–596
34. Korasick, D. A., Enders, T. A., and Strader, L. C. (2013) Auxin biosynthesis and storage forms. *J. Exp. Bot.* **64,** 2541–2555
35. Novák, O., Hényková, E., Sairanen, I., Kowalczyk, M., Pospíšil, T., and Ljung, K. (2012) Tissue-specific profiling of the *Arabidopsis thaliana*

auxin metabolome. *Plant J.* **72,** 523–536

36. Kai, K., Horita, J., Wakasa, K., and Miyagawa, H. (2007) Three oxidative metabolites of indole-3-acetic acid from *Arabidopsis thaliana*. *Phytochemistry* **68,** 1651–1663

37. Pencík, A., Simonovik, B., Petersson, S. V., Henyková, E., Simon, S., Greenham, K., Zhang, Y., Kowalczyk, M., Estelle, M., Zažímalová, E., Novák, O., Sandberg, G., and Ljung, K. (2013) Regulation of auxin homeostasis and gradients in *Arabidopsis* roots through the formation of the indole-3-acetic acid catabolite 2-oxindole-3-acetic acid. *Plant Cell* **25,** 3858–3870

38. Benjamins, R., and Scheres, B. (2008) Auxin: the looping star in plant development. *Annu. Rev. Plant Biol.* **59,** 443–465

39. Vanneste, S., and Friml, J. (2009) Auxin: a trigger for change in plant development. *Cell* **136,** 1005–1016

40. Habets, M. E. J., and Offringa, R. (2014) PIN-driven polar auxin transport in plant developmental plasticity: a key target for environmental and endogenous signals. *New Phytol.* **203,** 362–377

41. Runions, A., Smith, R., and Prusinkiewicz, P. (2014) Computational models of auxin-driven development. in *Auxin and its role in plant development* (Zažímalová, E., Petrášek, J., and Benková, E. eds.), Springer, Vienna. pp 315–357

42. Peer, W. A., Cheng, Y., and Murphy, A. S. (2013) Evidence of oxidative attenuation of auxin signalling. *J. Exp. Bot.* **64,** 2629–2639

43. Diet, A., Link, B., Seifert, G. J., Schellenberg, B., Wagner, U., Pauly, M., Reiter, W. D., and Ringli, C. (2006) The *Arabidopsis* root hair cell wall formation mutant *lrx1* is suppressed by mutations in the *RHM1* gene encoding a UDP-L-rhamnose synthase. *Plant Cell* **18,** 1630–1641

44. Kuhn, B. M., Geisler, M., Bigler, L., and Ringli, C. (2011) Flavonols accumulate asymmetrically and affect auxin transport in *Arabidopsis*. *Plant Physiol.* **156,** 585–595

45. Reiter, W. D., and Vanzin, G. F. (2001) Molecular genetics of nucleotide sugar interconversion pathways in plants. *Plant. Mol. Biol.* **47,** 95–113

46. Leiber, R.-M., John, F., Verhertbruggen, Y., Diet, A., Knox, J. P., and Ringli, C. (2010) The TOR pathway modulates the structure of cell walls in *Arabidopsis*. *Plant Cell* **22,** 1898–1908

47. Stintzi, A., and Browse, J. (2000) The *Arabidopsis* male-sterile mutant, *opr3*, lacks the 12-oxophytodienoic acid reductase required for jasmonate synthesis. *Proc. Natl. Acad. Sci. U.S.A.* **97,** 10625–10630

48. Horiguchi, G., Fujikura, U., Ferjani, A., Ishikawa, N., and Tsukaya, H. (2006) Large-scale histological analysis of leaf mutants using two simple leaf observation methods: identification of novel genetic pathways governing the size and shape of leaves. *Plant J.* **48,** 638–644

49. Geisler, M., Blakeslee, J. J., Bouchard, R., Lee, O. R., Vincenzetti, V., Bandyopadhyay, A., Titapiwatanakun, B., Peer, W. A., Bailly, A., Richards, E. L., Ejenda, K. F. K., Smith, A. P., Baroux, C., Grossniklaus, U., Müller, A., Hrycyna, C. A., Dudler, R., Murphy, A. S., and Martinoia, E. (2005) Cellular efflux of auxin catalyzed by the *Arabidopsis* MDR/PGP transporter At-PGP1. *Plant J.* **44,** 179–194

50. Geisler, M., Kolukisaoglu, H. U., Bouchard, R., Billion, K., Berger, J., Saal, B., Frangne, N., Koncz-Kalman, Z., Koncz, C., Dudler, R., Blakeslee, J. J., Murphy, A. S., Martinoia, E., and Schulz, B. (2003) TWISTED DWARF1, a unique plasma membrane-anchored immunophilin-like protein, interacts with *Arabidopsis* multidrug resistance-like transporters AtPGP1 and AtPGP19. *Mol. Biol. Cell* **14,** 4238–4249

51. Lewis, D. R., and Muday, G. K. (2009) Measurement of auxin transport in *Arabidopsis thaliana*. *Nat. Protoc.* **4,** 437–451

52. Dobrev, P. I., and Kamínek, M. (2002) Fast and efficient separation of cytokinins from auxin and abscisic acid and their purification using mixed-mode solid-phase extraction. *J. Chromatogr. A* **950,** 21–29

53. Dobrev, P. I., and Vankova, R. (2012) Quantification of abscisic acid, cytokinin, and auxin content in salt-stressed plant tissues. *Methods Mol. Biol.* **913,** 251–261

54. Shao, H., He, X., Achnine, L., Blount, J. W., Dixon, R. A., and Wang, X. (2005) Crystal structures of a multifunctional triterpene/flavonoid glycosyltransferase from Medicago truncatula. *Plant Cell* **17,** 3141–3154

55. Offen, W., Martinez-Fleites, C., Yang, M., Kiat-Lim, E., Davis, B. G., Tarling, C. A., Ford, C. M., Bowles, D. J., and Davies, G. J. (2006) Structure of a flavonoid glucosyltransferase reveals the basis for plant natural product modification. *EMBO J.* **25,** 1396–1405

56. Osmani, S. A., Bak, S., and Møller, B. L. (2009) Substrate specificity of plant UDP-dependent glycosyltransferases predicted from crystal structures and homology modeling. *Phytochemistry* **70,** 325–347

57. Butelli, E., Titta, L., Giorgio, M., Mock, H.-P., Matros, A., Peterek, S., Schijlen, E. G. W. M., Hall, R. D., Bovy, A. G., Luo, J., and Martin, C. (2008) Enrichment of tomato fruit with health-promoting anthocyanins by expression of select transcription factors. *Nat. Biotechnol.* **26,** 1301–1308

58. Buer, C. S., Kordbacheh, F., Truong, T. T., Hocart, C. H., and Djordjevic, M. A. (2013) Alteration of flavonoid accumulation patterns in *transparent testa* mutants disturbs auxin transport, gravity responses, and imparts long-term effects on root and shoot architecture. *Planta* **238,** 171–189

59. Lewis, D. R., Ramirez, M. V., Miller, N. D., Vallabhaneni, P., Ray, W. K., Helm, R. F., Winkel, B. S. J., and Muday, G. K. (2011) Auxin and ethylene induce flavonol accumulation through distinct transcriptional networks. *Plant Physiol.* **156,** 144–164

60. Woodward, A. W., and Bartel, B. (2005) Auxin: Regulation, action, and interaction. *Ann. Bot.* **95,** 707–735

61. Rampey, R. A., LeClere, S., Kowalczyk, M., Ljung, K., Sandberg, G., and Bartel, B. (2004) A family of auxin-conjugate hydrolases that contributes to free indole-3-acetic acid levels during *Arabidopsis* germination. *Plant Physiol.* **135,** 978–988

62. Spiess, G. M., Hausman, A., Yu, P., Cohen, J. D., Rampey, R. A., and Zolman, B. K. (2014) Auxin input pathway disruptions are mitigated by changes in auxin biosynthetic gene expression in *Arabidopsis*. *Plant Physiol.* **165,** 1092–1104